

## Article

# Diagnostic relations between pressure and entropy perturbations for acoustic and entropy modes

Sergey Leble<sup>1,‡\*</sup> and Ekaterina Smirnova<sup>1,‡</sup> 

<sup>1</sup> Immanuel Kant Baltic Federal University, Kaliningrad, Kaliningrad Oblast 236041, Russia;

\* Correspondence: lebleu@mail.ru

‡ These authors contributed equally to this work.

**Abstract:** Diagnostics and decomposition of atmospheric disturbances in a planar flow are considered and applied to numerical modeling results with the direct possibility to use in atmosphere monitoring especially in such strong events which follow magnetic storms and other large scale atmospheric phenomena. The study examines a situation in which the stationary equilibrium temperature of a gas may depend on a vertical coordinate, that seriously complicates the problem solution. The relations connecting perturbations for acoustic and entropy (stationary) modes are analytically established and led to the solvable diagnostic equations. These perturbation structures, found as the equation solutions specify acoustic and entropy modes in an arbitrary stratified gas under the condition of stability. These time-independent diagnostic relations link gas perturbation variables of the acoustic and the entropy modes. Hence, they provide the ability to decompose the total vector of perturbations into acoustic and non-acoustic (entropy) parts uniquely at any instant within the all accessible heights range. As a prospective model, we consider the diagnostics at the height interval 120-180 km, where the equilibrium temperature of a gas depends linearly on the vertical coordinate. For such a heights range it is possible to proceed with analytical expressions for pressure and entropy perturbations of gas variables. Individual profiles of acoustic and entropy parts for some data, obtained by numerical experiment, are illustrated by the plots for the pure numerical data against ones obtained by the model. The total energy of a flow is determined for both approaches and its height profiles are compared.

**Keywords:** acoustics of non-uniform media, wave mode diagnostics, entropy mode, initialization of hydrodynamic field

## 1. Introduction

Theoretical and numerical models, that describe dynamics of gases and liquids affected by external forces are of great interest in geophysics, meteorology, and wave theory [1-6]. The external forces and sources of energy, as well as momentum transfer, make the background of a fluid non-uniform. Hence, equilibrium thermodynamic parameters should depend on spatial coordinates. It drastically complicates the definition of linear modes (motions of infinitely small magnitude) taking place in such non-uniform media, so-called "non-exponential". The number of roots of the dispersion equation, if it is possible to determine them, agrees with the number of types of motion, and equals the number of balance equations [4]. Each of the balance equations represents a partial differential equation (PDE) which contains the first-order derivative with respect to time. In the case of isothermal gas in equilibrium with pressure and density depending exponentially on the coordinate (named often the "exponential atmosphere"), and in the simplest case of a planar flow, the dispersion relations may be introduced over the total wavelength range. Such a model is widely used for the classification of wave modes in practice as a "zero approximation". The realistic non-exponential case needs either consideration of the atmosphere as a layered medium or, for the short waves, making use of the Wentzel, Kramers, Brillouin (WKB) method [3]. Generally, such sources as

tsunami, lying at the bottom of the Atmosphere excite combined waves with the leading front formed by quasiplane acoustics [7].

There are three types of motion in a one-dimensional (1D) exponential atmosphere: two acoustic modes of different direction of propagation, and the entropy mode, corresponding to zero frequency for a linear lossless flow [1,2]. The entropy mode, however, is not stationary in a viscous fluid that conducts heat, and with a non-linearity account [1,4,8]. In the flows exceeding one dimension, the buoyancy, or "internal" waves appear [3,4]. For Rossby and Poincare waves description see, e.g. [4,6] The first results that allow distinguishing modes due to relations of specific perturbations have been obtained namely relative to the motion of an exponentially stratified ideal gas in the constant gravitational field [6,8,10]. Mathematically, such relations are fixed as ones of eigenvectors and corresponding projecting operators of the evolution operator, defined by the basic balance system.

Experimental observation of wave and non-wave disturbances is not easy, there are special facilities as "Sura" [11] based on the active experiment of ionosphere excitation that allows measuring directly the atmosphere parameters variations at the ionosphere heights [12]. Only recently an attempt to apply the diagnostic method, based on projecting operators technique, was realized within a set of such measurements. The projecting technique was developed for a space-evolution operator, that allows to apply it to atmosphere parameters relations at a vicinity of a point of observation. It allowed to distinguish up- and down- directed acoustic wave via the real dataset [13], in this work the algorithm of entropy mode diagnosis was elaborated, see also [14].

This work considers the dynamics of ideal atmosphere gas perturbations over a background of equilibrium temperature, dependent on height, affected by a gravitational field and other geophysical impacts. The main aim of this study is the diagnostics as decomposition of a disturbance to wave and non-wave modes in the case of arbitrary stable stratification. This is helpful in the interpretation of experimental data related to the significantly disturbed atmosphere (e.g. by storms), it also may be useful in a validation of a numerical modelling [15]. Especially, it is important in establishing the location of wave sources, and modelling the atmosphere's warming [16,17], related to the atmosphere gas wave heating. The theory should base on the balance equations and rely upon physically justified boundary conditions and simplifications [18], its mode decomposition should be instructive in a specific mathematical statement of problem formulation [19,20].

In this study, which develops ideas of [21], the modes of a planar flow are determined by means of relations between specific perturbations that are time-independent. We name such relations as "*diagnostic relations*". They are valid for arbitrary dependence of the equilibrium temperature on a coordinate for the case of a stable atmosphere. These relations give the ability to distinguish modes from the total field analytically at any instant, solving the *diagnostic equations*, that are the direct corollary of the mentioned diagnostic relations. It serves as a tool to predict their dynamics, and to conclude about the energy of modes (which remains constant in time). This is undoubtedly important in applications in meteorology and diagnostics of atmospheric dynamics, including the understanding of such phenomena as variations of the equilibrium temperature of the stratosphere, e.g. so-called warming [22] conventionally understood as period-average. Such phenomenon may be explained in the framework of non-linear interaction of acoustic wave and entropy modes in presence of a dissipation [17,23], named as "heating" in laboratory acoustics. The whole exposition is also important in the diagnostics of wave and non-wave modes in order to follow experimental observations and numerical simulations [15] as an element of atmosphere dynamics monitoring [9]. The authors of [9] stress, that the acoustic component of a perturbation is the first that reach ionosphere heights, that is important for the mentioned hazard phenomena detection.

As the practical example of the general theory and the particular model applications we use the dataset of numerical modelling of an atmospheric perturbation by

the source, positioned at the vicinity of Earth surface [18],[19]. The theory uses the standard atmosphere  $H(z)$  profile [24] at the  $z \in [0, 500]$  km range with the application of diagnostic equations solution with the right-hand-side (RHS), discretized as the dataset from a numerical experiment we use. We, however, should omit intervals of instability with non-positive energy density. To proceed we choose a diagnostic at the interval at which the  $H(z)$  profile is well approximated by a linear function. It is the heights range  $z \in [120, 180]$  km, for which we elaborate the model with the explicit form of the diagnostic equation solution. For such interval, we compare the results of the general theory digitization and the result of a more compact model, based on explicit approximation of the  $H(z)$  profile at the pointed height range.

We begin from the basic system of balance equations and derive the diagnostic ones (Sec. 2). In the final subsection, we solve the differential diagnostic equation by the method of factorization. Next, we apply the obtained relation to the datasets, obtained by numerical solution of an atmosphere perturbation problem [18] within the heights range  $z \in [120, 180]$  km, using the  $H(z)$  profile from standard atmosphere [24]. It results in entropy mode contribution profiles (Sec. 5). In the Sec. 5.2 we build the model for the mentioned heights interval repeating the calculations, when possible, analytically, see also [25]. The results, obtained by the direct applications of the theory to the dataset on the base of the standard atmosphere profile within the range of approximate linearity and the model results are compared.

## 2. Diagnostic relations

### 2.1. Basic balance equations for arbitrary stable stratification

The case of the non-exponential atmosphere in equilibrium permits to fix the entropy and acoustic mode without subdivision into "upwards" and "downwards" directed acoustic waves [21], see also [10]. The main functional parameter in this case, the local *atmosphere's scale height*  $H(z)$  depends on height as, e.g. in [24]. The background density which supports the equilibrium distribution of temperature  $\bar{T}(z)$ , takes the form:

$$\bar{\rho}(z) = \frac{\bar{\rho}(0)H(0)}{H(z)} \exp\left(-\int_0^z \frac{dz'}{H(z')}\right), \quad (1)$$

where the pressure scale height is

$$H(z) = \frac{\bar{p}}{\bar{\rho}g} = \frac{\bar{T}(z)(C_p - C_v)}{g}. \quad (2)$$

Here the conventional gas parameters are used:  $g$  - gravity acceleration,  $C_{p,v}$  are the molar heat capacities at constant  $p,v$  correspondingly. It is convenient to introduce the quantity  $\varphi'$  instead of perturbation in density

$$\varphi' = p' - \gamma \frac{\bar{p}}{\bar{\rho}} \rho', \quad (3)$$

where the parameter  $\gamma = C_p/C_v$ . We will name it the entropy perturbation, because in a limit with  $g = 0$  and constant background temperature  $\bar{T}$ ,  $\varphi'$  represents the deviation of the ideal gas entropy from the equilibrium one [27].

As it was done in [25] we use the conventional set of variables:

$$P = p' \cdot \exp\left(\int_0^z \frac{dz'}{2H(z')}\right), \quad (4)$$

$$\Phi = \varphi' \cdot \exp\left(\int_0^z \frac{dz'}{2H(z')}\right), \quad (5)$$

$$U = V \cdot \exp \left( - \int_0^z \frac{dz'}{2H(z')} \right), \quad (6)$$

where  $P, \Phi, U$  are the new quantities defined in this way (Eqs, (4,5,6)) and  $V$  is the vertical velocity of the flow. The system of momentum-energy-mass balance equations in new variables reads (see [10,25]):

$$\frac{\partial U}{\partial t} = \frac{1}{\bar{\rho}(0)} \left( \frac{\gamma - 2}{2\gamma H(0)} - \frac{H(z)}{H(0)} \frac{\partial}{\partial z} \right) P + \frac{\Phi}{\gamma H(0) \bar{\rho}(0)}, \quad (7)$$

$$\frac{\partial P}{\partial t} = -\gamma g H(0) \bar{\rho}(0) \frac{\partial U}{\partial z} - g H(0) \bar{\rho}(0) \frac{\gamma - 2}{2H(z)} U, \quad (8)$$

$$\frac{\partial \Phi}{\partial t} = -\frac{\nu(z)}{H(z)} g H(0) \bar{\rho}(0) U, \quad (9)$$

where  $\nu(z)$  is positive:

$$\nu(z) = \gamma - 1 + \gamma \frac{dH(z)}{dz} > 0, \quad (10)$$

that guarantee the positive definition of energy density, defined at the Sec. 6.

## 2.2. Relation between pressure and entropy perturbations for acoustic and entropy modes

The relation that links the pressure and entropy perturbation within the acoustic mode, for arbitrary stable stratification of 1D atmosphere can be obtained by substituting the Eq.(9) into the Eq.(8) [25]. As a result, the *diagnostic relation* between the pressure and entropy perturbations within the acoustic mode follows:

$$P_a = \left( \frac{\gamma - 2}{2\nu(z)} + \gamma \frac{\partial}{\partial z} \frac{H(z)}{\nu(z)} \right) \Phi_a. \quad (11)$$

The first equation in the basic system (7) for  $U_0 = 0$  fixes the diagnostic link in the stationary (entropy) mode:

$$\Phi_0 = \left( -\frac{\gamma - 2}{2} + \gamma H(z) \frac{\partial}{\partial z} \right) P_0. \quad (12)$$

The relations (11) and (12) can be rewritten as

$$P_a + D_a \Phi_a = 0, \quad (13)$$

$$\Phi_0 + D_0 P_0 = 0, \quad (14)$$

where the operators

$$D_a = - \left( \frac{\gamma - 2}{2\nu(z)} + \gamma \frac{\partial}{\partial z} \frac{H(z)}{\nu(z)} \right), \quad (15)$$

$$D_0 = - \left( -\frac{\gamma - 2}{2} + \gamma H(z) \frac{\partial}{\partial z} \right) \quad (16)$$

are the first order differential operators. We name the Eqs.(13,14) as *diagnostic relations*, that define the acoustic and entropy mode in the 1D atmosphere with arbitrary stratification.

## 2.3. Diagnostic equations

Let us introduce operator-valued two-component vector:

$$( 1 \quad D_a ), \quad (17)$$

and the column that represents the vector of state:

$$\begin{pmatrix} P \\ \Phi \end{pmatrix}, \quad (18)$$

where

$$P = P_a + P_0, \Phi = \Phi_a + \Phi_0. \quad (19)$$

The action

$$\begin{pmatrix} 1 & D_a \end{pmatrix} \begin{pmatrix} P \\ \Phi \end{pmatrix} = P + D_a \Phi = P_a + D_a \Phi_a + P_0 + D_a \Phi_0 = P_0 + D_a \Phi_0 = P_0 - D_a D_0 P_0, \quad (20)$$

defines the second order ordinary differential equation, we would name as the *diagnostic* one:

$$(1 - D_a D_0) P_0 = P + D_a \Phi = f_0(z). \quad (21)$$

So, to extract the entropy mode, we need to solve the differential equation (21) with appropriate boundary conditions. Similar consideration with a solution form is presented at [21] in different units. The acoustic mode either could be extracted in the same manner or simply using the identity  $P = P_a + P_0$ .

There is also a similar alternative, which also leads to a second order differential diagnostic equation but for  $P_a$ . This alternative is implemented by the action of the row operator vector on the column vector function

$$\begin{pmatrix} D_0 & 1 \end{pmatrix} \begin{pmatrix} P \\ \Phi \end{pmatrix} = D_0 P + \Phi = D_0 P_a + \Phi_a + D_0 P_0 + \Phi_0 = D_0 P_a + \Phi_a = -D_a^{-1} P_a + D_0 P_a = (D_0 - D_a^{-1}) P_a. \quad (22)$$

The diagnostic relation (14) is taken into account. The derivation results in the second order equation

$$D_a D_0 P_a - P_a = f_a(z) = D_a D_0 P + D_a \Phi \quad (23)$$

see also [25], where the derivation is absent. The operator at the LHS of the *second diagnostic equation* (23) transforms as

$$D_a D_0 - 1 = \left( \frac{\gamma - 2}{2\nu(z)} + \gamma \frac{\partial}{\partial z} \frac{H(z)}{\nu(z)} \right) \left( -\frac{\gamma - 2}{2} + \gamma H(z) \frac{\partial}{\partial z} \right) - 1. \quad (24)$$

### 3. On the dataset

We process the set of numerical experiment data consisting of horizontal coordinate, vertical coordinate, pressure, background pressure, density, background density, temperature, wave perturbation of temperature, wave perturbation of pressure, wave perturbation of density. The mentioned physical values are given as files such that for the fixed horizontal coordinate the vertical coordinate  $z_i$  is presented for the range [0,500] km with the steps that varies with a height difference from 150 m to 2000 m. The fixed time and horizontal coordinate seem to be convenient since the one-dimensional theory is considered. Data set was provided to authors by the sources, related to the paper [19]. The model, used in this paper [29], is a numeric solution of the full two-dimensional non-linear system of hydrothermodynamic balance equations. The program that processes the dataset allows solving the diagnostic equations (21,23) with reasonable accuracy of about a few percents, as estimated by the Runge rule.

According to the equations rhs (21,23) and the diagnostic equations (14,13), such a study requires pressure and entropy data for constructing function  $f_0(z), f_a(z)$ , where the link of the variables  $P, \Phi$  with original, pressure and density wave perturbations  $p'$  and  $\rho'$  directly measured or calculated ones, are described by the relations (4) and (5).

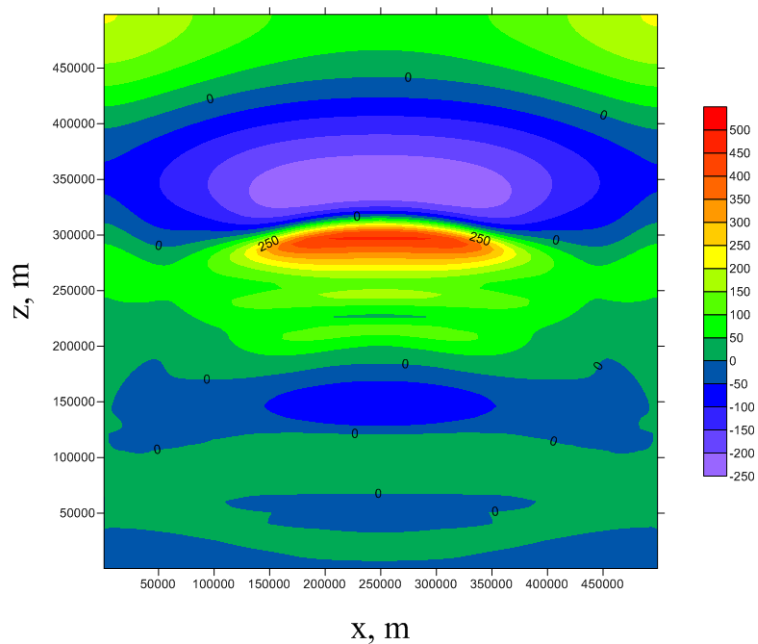


**Figure 1.** Wave perturbation of temperature from a local source of pressure fluctuations for the considered moment of time. Result of numeric modeling [19]. Courtesy of. Yu. Kurdjaeva.

### 3.1. Standard atmosphere $H(z)$ profile

In this section we prepare the atmosphere characteristics for numerical calculations, starting from the atmospheric scale height calculated as

$$H(z_i) = H_i = \frac{R_s T(z_i)}{g}, \quad (25)$$

where  $z_i$  -  $i$ -row element of the discrete data array for vertical coordinate,  $H_i$  - the value of the atmosphere scale height at the height  $z_i$ ,  $T(z_i)$  - the value of the temperature at the reference height  $z_i$ ,  $R_s = R/M = 287.1 \text{ J/(kg}\cdot\text{K)}$  - the specific gas constant for dry air [24]. The height scale profile is built directly by the table for background temperature

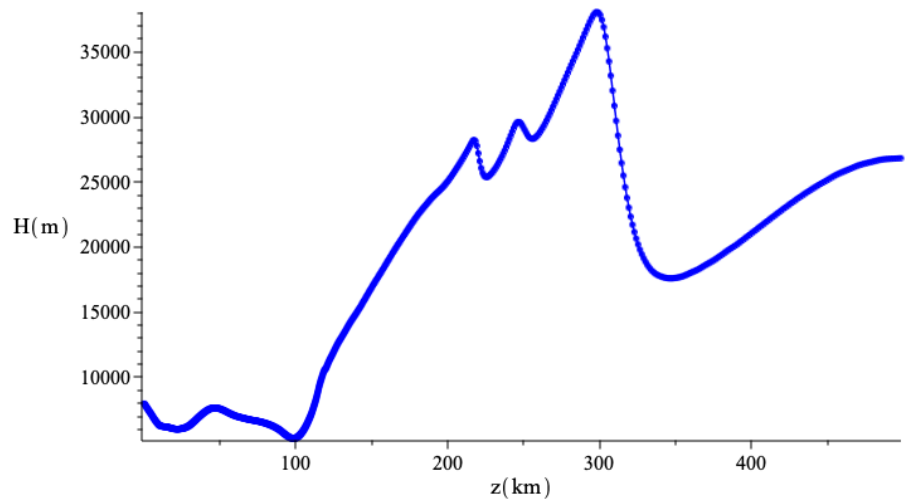


**Figure 2.** The height scale  $H(z_i)$  profile obtained according to the formula (25) [24].

$T(z_i)$ , taken from [24]. The function (10) we approximate as follows

$$\nu_i(z_i) = \gamma - 1 + \gamma \frac{dH(z)}{dz} \Big|_{z=z_i} \approx \gamma - 1 + \gamma \frac{H_{i+1} - H_{i-1}}{z_{i+1} - z_{i-1}}. \quad (26)$$

The expression shows how we estimate the derivatives (excluding the first and last points, where the left and right derivatives approximations are used).

### 3.2. Linear approximation of $H(z)$

According to the graph for the atmosphere's scale height in Fig.2, we will focus on the approximately linear part in the interval  $z \in [120; 180]$  km.

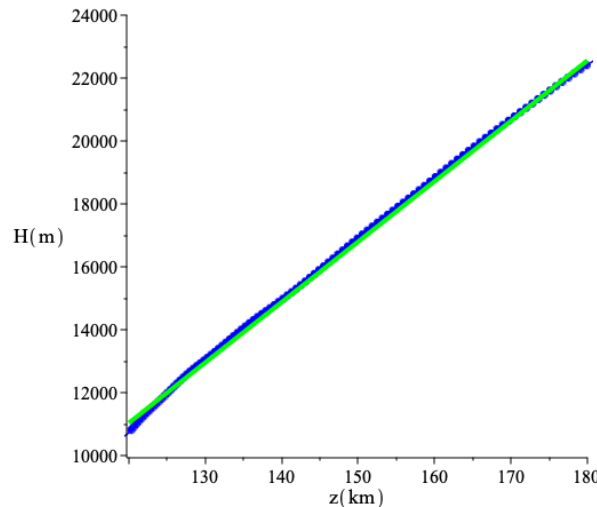


**Figure 3.** Standard atmosphere  $H(z_i)$  for  $z_i$  within 120 km to 180 km range (in blue) and its linear approximation represented by formula (27) (in green)

Note, that the difference between the dependence of  $H(z)$  taken from the dataset and the linear approximations, given in Fig. 3 within 120 km to 180 km range, is almost invisible at such scale. This gives an argument to use such linear approximation in further modelling. To provide the model test, we put  $H(z)$  depending linearly on the coordinate  $z$  like:

$$H(z) = \alpha z - H \quad (27)$$

where the curves at the Figure 3 adjustment is provided by the following choice

$$H = 12000 \text{ m}, \quad (28)$$

$$\alpha = 0.192. \quad (29)$$

The function  $H(z) = 0.192z - 12000$  graph is shown in red in Fig.3.

For the linear  $H(z)$  case the function (10) is:

$$\nu(z) = \gamma - 1 + \gamma \frac{dH(z)}{dz} = \gamma - 1 + \gamma \alpha. \quad (30)$$

#### 4. Solution of a diagnostic equation for linear dependence of $H(z)$ by factorization method

##### 4.1. Operator factorization

Let us choose the equation (21), where

$$1 - D_a D_0 = 1 - \gamma^2 \frac{(H(z))^2}{\nu(z)} \frac{\partial^2}{\partial z^2} - 2\alpha\gamma \cdot \gamma \frac{H(z)}{\nu(z)} \frac{\partial}{\partial z} + \frac{\gamma^2 + 2\alpha\gamma^2}{4\nu(z)}, \quad (31)$$

for the entropy mode  $(1 - D_a D_0)P_0 = f_0$ , or, on base of linear approximation of  $H(z)$ , it, by the factorization, writes by the following

$$(D^2 + ED - A)P_0 = (D - \phi)(D - \psi)P_0 = -(\gamma + \alpha\gamma - 1)f_0 = -\nu(z)f_0, \quad (32)$$

where, for the factorization convenience, the following expressions are introduced

$$D = \gamma H(z) \frac{\partial}{\partial z}, \quad E = \alpha\gamma, \quad A = \frac{\gamma^2 + 2\alpha\gamma^2}{4}, \quad (33)$$

$$\phi = E - \psi, \quad (34)$$

$$\psi = \frac{1}{2} \sqrt{E^2 + 4A} - \frac{1}{2}E. \quad (35)$$

The operator of the second diagnostic equation (23) for the acoustic mode is opposite to one of the first diagnostic equation, hence its solution differs only by the RHS (inhomogeneity).

##### 4.2. On boundary conditions

###### 4.2.1. General remarks. Diagnosis.

A statement of the problem for the second order equations as (21,23) implies two boundary conditions either at the ends of the interval of consideration or both at one end of the heights range.

Generally, the inhomogeneous equation with the linear operator  $A$

$$Au = f_0 \quad (36)$$

is solved up to general solution of the homogeneous one:

$$u = A^{-1}f_0 + u_h, \quad (37)$$

$$Au_h = 0. \quad (38)$$

The function  $u_h$  is fixed by a set of boundary condition. In the case of the second order differential equation, we should choose two such conditions that determine the constants  $C, C_1$ .

In the problem of diagnostics, its formulation is more complicated. We have two ODE for the variables  $P_0$  and  $P_a$  of the same form of the operator, but with different RHS, The statement of the problem should also keep the condition

$$P_0 + P_a = P, \quad (39)$$

within the whole range of the problem including the boundary.

###### 4.2.2. Boundary problem.

The condition (39) being read literally, impose the condition

$$P_a(z_2) = P(z_2) - P_0(z_2). \quad (40)$$

It, together with

$$P_0(z_1) = 0, \quad P'_0(z_1) = 0, \quad (41)$$

and

$$P_a(z_1) = P(z_1). \quad (42)$$

closes the diagnostics problem formulation we investigate within this work.

#### 4.3. Solution of the first and second diagnostic equations

The general solution of the equation (32) formally reads as

$$P_0 = (1 - D_a D_0)^{-1} (P + D_0 \Phi). \quad (43)$$

It is found by the conventional factorization of the first order operators at (32). We write the solution as

$$P_0 = -\frac{(\gamma + \alpha\gamma - 1)}{\gamma^2} S \int_{z_1}^z \frac{T}{SZ} \int_{z_1}^{z''} \frac{f_0}{TZ} dz' dz'' + \frac{CS}{\gamma} \int_{z_1}^z \frac{T}{SZ} dz' + C_1 S, \quad (44)$$

where  $S = Z^{\frac{1}{\alpha\gamma}(-\frac{1}{2}E + \frac{1}{2}\sqrt{E^2 + 4A})} = Z^a$ ,  $T = Z^{-\frac{1}{\alpha\gamma}(\frac{1}{2}E + \frac{1}{2}\sqrt{E^2 + 4A})} = Z^b$ ,  $Z = \alpha z + H$ .

Thinking about the entropy mode presence as a result of the heating by a wave propagating from the bottom end of the interval  $z \in [z_1, z_2]$ , we choose the pair of conditions for the entropy mode variable  $P_0$  and its derivative

$$P_0(z_1) = 0, \quad P'_0(z_1) = 0, \quad (45)$$

that mimics an (approximate) absence of the entropy mode at a vicinity of the lower point  $z_1$ . The second condition of (45) responds to the diagnostic relation (14), i.e.  $\Phi_0 = 0$ .

In such a case the conditions for the acoustic component looks

$$P_a(z_1) = P(z_1). \quad (46)$$

The boundary values in the (46) are taken either from an experiment or from a dataset obtained from numerical modeling.

The constants of integration  $C, C_1$  are defined from the boundary conditions (45).  $C_1$  is determined by the condition

$$P(z_1) = C_1 Z(\alpha z_1 - H)^a = 0, \quad (47)$$

therefore  $C_1 = 0$ , i.e.

$$P_0 = -\frac{(\gamma + \alpha\gamma - 1)}{\gamma^2} S \int_{z_1}^z \frac{T}{SZ} \int_{z_1}^{z''} \frac{f_0}{TZ} dz' dz'' + \frac{CS}{\gamma} \int_{z_1}^z \frac{T}{SZ} dz'. \quad (48)$$

The second condition at  $z_1$ , the relation (45), gives for the derivative the following,

$$P'_0 = -\frac{\gamma + \alpha\gamma - 1}{\gamma^2} \left( S' \int_{z_1}^z \frac{T}{SZ} \int_{z_1}^{z''} \frac{f_0}{TZ} dz' dz'' + \frac{T}{SZ} \int_{z_1}^z \frac{f_0}{TZ} dz' dz'' \right) + \frac{CS'}{\gamma} \int_{z_1}^z \frac{T}{SZ} dz' + \frac{C}{\gamma} \frac{T}{Z}. \quad (49)$$

Plugging  $z = z_1$  gives

$$P'_0(z_1) = \frac{C}{\gamma} \frac{T}{Z} = \frac{C}{\gamma} \frac{(\alpha z_1 - H)^{-\frac{1}{\alpha\gamma}(\frac{1}{2}E + \frac{1}{2}\sqrt{E^2 + 4A})}}{(\alpha z_1 - H)} = 0, \quad (50)$$

hence, the constant  $C$  is also zero.

Very similar, the second diagnostic equation (23) is solved as

$$P_a = -(1 - D_a D_0)^{-1} (D_a D_0 P + D_a \Phi) = (1 - D_a D_0)^{-1} (-f_a). \quad (51)$$

Subtracting the equations (21) and (23) yields

$$P_0 + P_a = (1 - D_a D_0)^{-1} (f_0 - f_a) = (1 - D_a D_0)^{-1} (P + D_a \Phi - D_a D_0 P - D_a \Phi) = P, \quad (52)$$

this identity is convenient for the solutions test.

The expression for  $P_a$  differs from (44) by the source ( $f_a$ ) and by the constants of integration, that gives

$$P_a = \frac{(\gamma + \alpha\gamma - 1)}{\gamma^2} S \int_{z_1}^z \frac{T}{S\bar{Z}} \int_{z_1}^{z''} \frac{f_a}{T\bar{Z}} dz' dz'' + \frac{C'S}{\gamma} \int_{z_1}^z \frac{T}{S\bar{Z}} dz' + C'_1 S. \quad (53)$$

From the boundary conditions (46) it follows

$$P_a(z_1) = C'_1 S(z_1) = P(z_1). \quad (54)$$

The coefficients  $C'$  and  $C'_1$  are expressed from the last two formulas. Finally:

$$P_a = \frac{\gamma + \alpha\gamma - 1}{\gamma^2} S \int_{z_1}^z \frac{T}{S\bar{Z}} \int_{z_1}^{z''} \frac{f_a}{T\bar{Z}} dz' dz'' + \frac{P'(z_1)Z(z_1)}{T(z_1)} S \int_{z_1}^z \frac{T}{S\bar{Z}} dz' + \frac{P(z_1)}{S(z_1)} S. \quad (55)$$

#### 4.3.1. The second boundary problem. Acoustic mode

We left the first boundary condition for the acoustic mode

$$P_a(z_1) = C'_1 S(z_1) = P(0), \quad C'_1 = \frac{P(0)}{S(z_1)}. \quad (56)$$

The condition at the upper boundary is more complicated

$$P_a(z_2) = \frac{(\gamma + \alpha\gamma - 1)}{\gamma^2} S \int_{z_1}^{z_2} \frac{T}{S\bar{Z}} \int_{z_1}^{z''} \frac{f_a}{T\bar{Z}} dz' dz'' + \frac{C'S}{\gamma} \int_{z_1}^{z_2} \frac{T}{S\bar{Z}} dz' + \frac{P_a(0)}{S} S(z_2) \quad (57)$$

and at the same time

$$P_a(z_2) = P(z_2) - P_0(z_2), \quad (58)$$

that yields

$$C' = \frac{\frac{P(z_2) - P_0(z_2)}{S(z_2)} - \frac{\gamma + \alpha\gamma - 1}{\gamma^2} \int_{z_1}^{z_2} \frac{T}{S\bar{Z}} \int_{z_1}^{z''} \frac{f_a}{T\bar{Z}} dz' dz'' - \frac{P(0)}{S(z_1)}}{\frac{1}{\gamma} \int_{z_1}^{z_2} \frac{T}{S\bar{Z}} dz'}, \quad (59)$$

but guarantees the natural condition

$$P_a(z_2) + P_0(z_2) = P. \quad (60)$$

Note, that the entropy components of a disturbance are evaluated from the diagnostic relations:  $\Phi_0$  from (14) and the variable  $\Phi_a$  from (13).

## 5. Applications to data of a numeric experiment

### 5.1. Discrete representation of functions and operators for the standard atmosphere $H(z)$ case

From (21) we derive:

$$f_0(z_i) = P_i + D_{a,i}\Phi_i, \quad (61)$$

where according to the (15):

$$D_{a,i} = -\frac{\gamma-2}{2\nu_i(z_i)} - \gamma \frac{H_i}{\nu_i(z_i)} \frac{\partial}{\partial z} - \gamma \left( \frac{H(z)}{\nu_i(z)} \right)' \Big|_{z=z_i}. \quad (62)$$

In the same way the function (23)

$$f_a(z_i) = D_{a,i}D_{0,i}P_i + D_{a,i}\Phi_i \quad (63)$$

where according to the (16):

$$D_{0,i} = \frac{\gamma-2}{2} - \gamma H_i \frac{\partial}{\partial z}. \quad (64)$$

The functions  $P_i$  and  $\Phi_i$  are defined through a dataset using formulas (4),(5) that for the real  $H(z_i)$  case are:

$$P_i = P(z_i) = p'(z_i) \cdot \exp \left( \int_0^{z_i} \frac{dz'}{2H(z')} \right) \approx p'(z_i) \cdot \exp \left( \sum_{j=1}^i \frac{\Delta z_j}{2H(z_j)} \right), \quad (65)$$

$$\Phi_i = \Phi(z_i) = \varphi'(z_i) \cdot \exp \left( \int_0^{z_i} \frac{dz'}{2H(z')} \right) \approx \varphi'(z_i) \cdot \exp \left( \sum_{j=1}^i \frac{\Delta z_j}{2H(z_j)} \right). \quad (66)$$

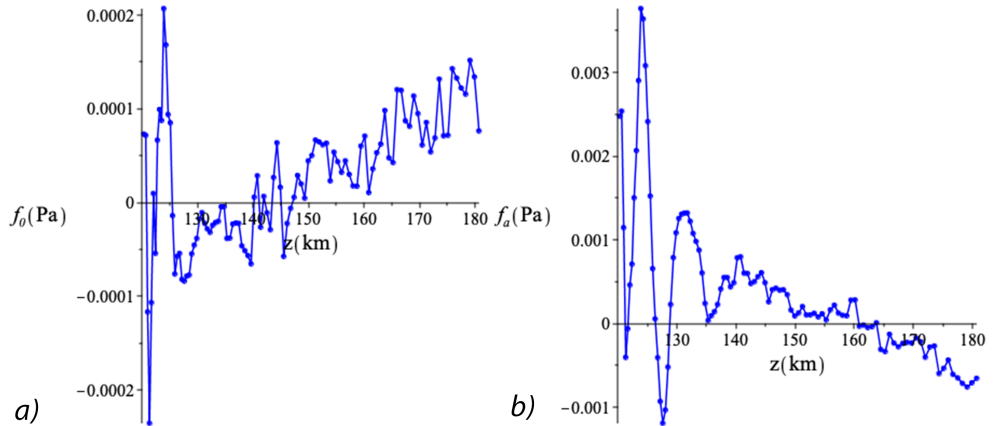


**Figure 4.** The plot a) is the graph of the function  $f_0(z_i)$  obtained by the formula (61) and the plot b) is the graph of  $f_a(z_i)$  obtained by the formula (63) for the case of standard atmosphere  $H(z_i)$  case represented by the formula (25).

The oscillations of the RHSs of the diagnostic equations for  $P_{0,a}$  (Figs 4), apart from a small variation of the functional parameter  $H(z)$ , appear due to the application of differentiation operation to the dataset components as in (62), which scale of coordinate differences and errors are noticeable.

It is seen at the Figs 5, that the result of the diagnosis as vertical structure of the contributions  $P_{0,a}$  in the pressure perturbation  $P$  looks much more smooth because its definition contains integration.

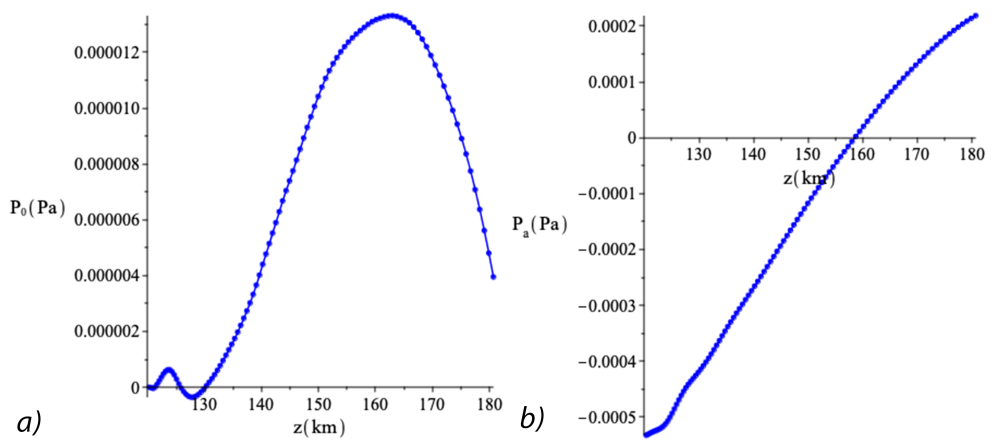


**Figure 5.** The plot a) is the graph of the solution  $P_0(z)$  obtained by the formula (44) and b) is the graph of the solution  $P_a(z)$  obtained by the formula (53) for the case of standard atmosphere  $H(z_i)$  case represented by the formula (25).

### 5.2. Representation of functions and operators for the linear $H(z)$ case

For linear approximation of  $H(z)$  of the form (27), the operators (15) and (16) have the form:

$$D_a = -\left( \frac{\gamma-2}{2(\gamma-1+\gamma\alpha)} + \gamma \frac{\partial}{\partial z} \frac{\alpha z - H}{\gamma-1+\gamma\alpha} \right), \quad (67)$$

$$D_0 = -\left( -\frac{\gamma-2}{2} + \gamma(\alpha z - H) \frac{\partial}{\partial z} \right). \quad (68)$$

For linear dependence of  $H(z)$  function  $f_0(z)$  from (21) can be calculated as:

$$f_0(z) = P + D_a \Phi = P - \frac{\gamma-2+2\alpha\gamma}{2(\gamma-1+\gamma\alpha)} \Phi - \frac{\gamma(\alpha z - H)}{\gamma-1+\gamma\alpha} \frac{\partial \Phi}{\partial z} \quad (69)$$

and function  $f_a(z)$  from (23):

$$f_a(z) = D_a D_0 P + D_a \Phi = \frac{1}{\gamma-1+\gamma\alpha} \left( -\frac{1}{4}(\gamma-2)(\gamma-2+2\alpha\gamma)P + \right. \quad (70)$$

$$\left. + 2\alpha\gamma^2(\alpha z - H) \frac{\partial P}{\partial z} + \gamma^2(\alpha z - H)^2 \frac{\partial^2 P}{\partial z^2} - \frac{1}{2}(\gamma-2+2\alpha\gamma)\Phi - \gamma(\alpha z - H) \frac{\partial \Phi}{\partial z} \right) \quad (71)$$

where pressure and entropy perturbation functions (4),(5) are:

$$P = p' \cdot \exp \left( \int_{z_1}^z \frac{dz'}{2H(z')} \right) = p' \cdot \exp \left( \frac{1}{2\alpha} (\ln(\alpha z - H) - \ln(\alpha z_1 - H)) \right), \quad (72)$$

$$\Phi = \varphi' \cdot \exp \left( \int_{z_1}^z \frac{dz'}{2H(z')} \right) = \varphi' \cdot \exp \left( \frac{1}{2\alpha} (\ln(\alpha z - H) - \ln(\alpha z_1 - H)) \right). \quad (73)$$

Here  $z_1$  - initial coordinate or in the case of a discrete dataset for the vertical coordinate, that yields:

$$P(z_i) = p' \cdot \exp \left( \frac{1}{2\alpha} (\ln(H(z_i)) - \ln(\alpha z_1 - H)) \right), \quad (74)$$

$$\Phi(z_i) = \varphi' \cdot \exp \left( \frac{1}{2\alpha} (\ln(H(z_i)) - \ln(\alpha z_1 - H)) \right). \quad (75)$$

We see, that the plots look as smooth as ones at Fig. 5. It is the result of the integration that acts as a "smoothing" operation, as opposite to differentiation. Such

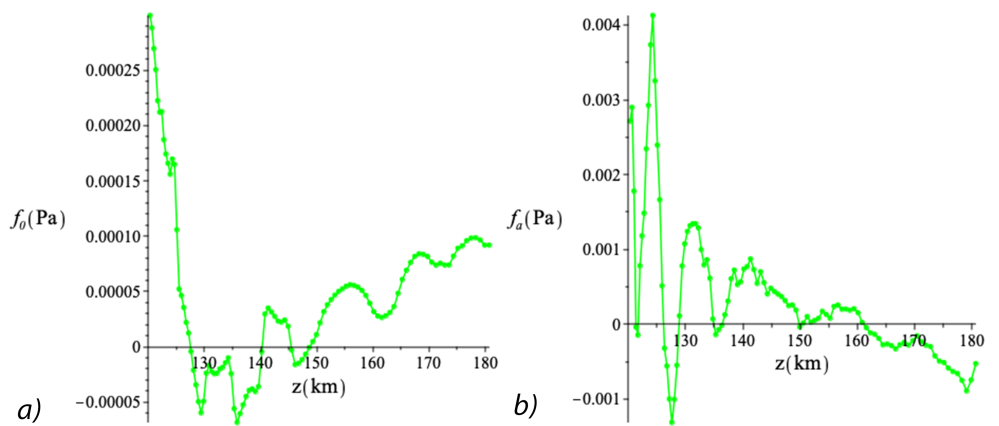


**Figure 6.** The plot a) is the graph of the function  $f_0(z)$  obtained by the formula (69) and the plot b) is the graph of  $f_a(z)$  obtained by the formula (71) for the case of linear dependence  $H(z)$  represented by the formula (27)

phenomena are well-known in the theory of inverse problems. The plots of the Fig 8

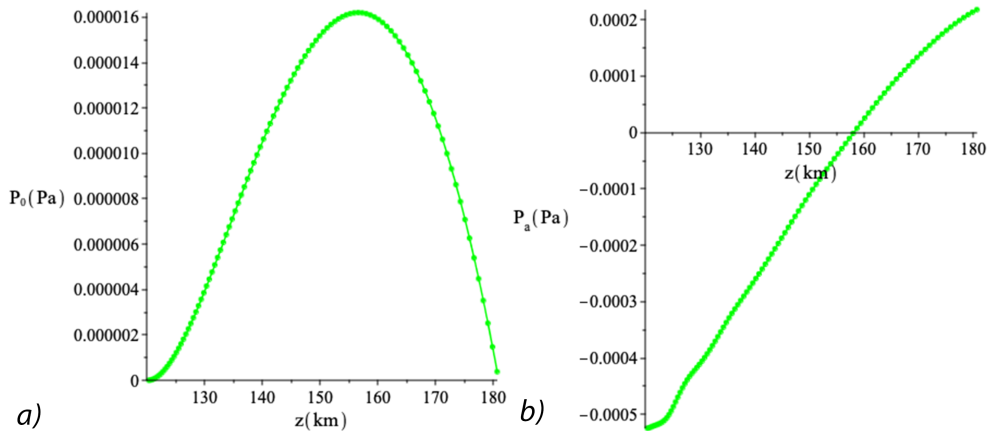


**Figure 7.** The plot a) is the graph of the solution  $P_0(z)$  obtained by the formula (44) and b) is the graph of the solution  $P_a(z)$  obtained by the formula (53) for the case of linear dependence  $H(z)$  represented by the formula (27)

represent one of the principal results of this work: it shows that there is a discrepancy between the profile obtained by the direct dataset processing and handling by means of the apparatus built by the analytical approximation of the theory elements. The difference, however, is not so big, the linear model allows to estimate the entropy mode profile. The transition to energy distribution leads to the results for which the difference almost disappear, see Fig. 9.

## 6. Comparison of the models and discussion of the results

The plots of the Fig 8 represent one of the principle result of this work: it shows that there is a discrepancy between the profile obtained by the direct dataset processing and handling by means of the apparatus built by the analytical approximation of the theory elements. The difference, however, is not so big, the linear model allows to estimate the entropy mode profile. The addition of independent results of calculations of  $P_0$  and  $P_a$  gives the curve closely matching with the graph of a function  $P$  represented by formula (4), which is consistent with the main idea of the expansion into modes  $P = P_0 + P_a$ . The transition to energy distribution leads to the results for which the difference almost disappear, see Fig. 9.

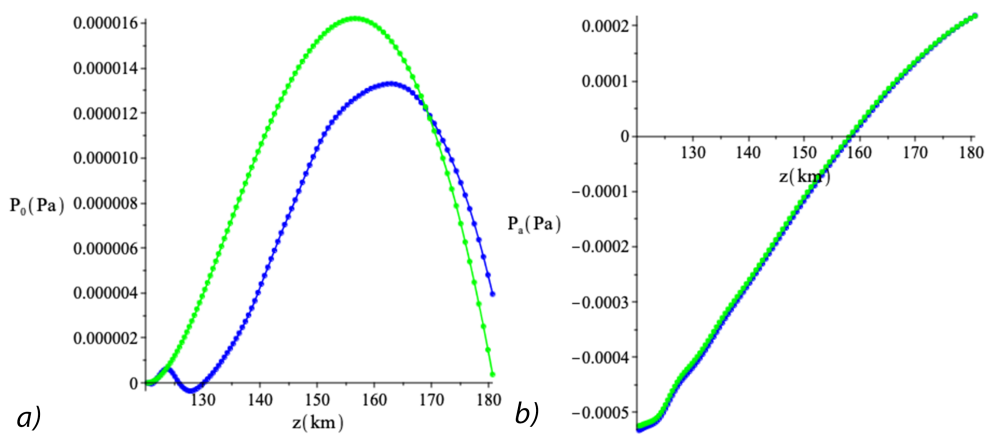


**Figure 8.** Comparison of the entropy mode  $P_0(z)$  (a) and the acoustic one  $P_a(z)$  (b) obtained using the formulas (44) and (53), respectively, for the cases of standard atmosphere  $H(z)$  (25) (in blue) and linear height scale dependence  $H(z)$  model (27) (in green).

The authors believe that the analytical models are more desirable than numerical methods, which are usually time-consuming, require a high-performance computer, and special attention to underlying algorithms, their convergence, and stability investigation. On the other hand, reasonably simple analytical models also, when complemented by a numerical approach, are much more efficient.

Speaking about the modes extraction at the level of the pressure-entropy vector disturbances field we observe the difference of the results, visible at the plots of the Figure 8. The difference (by module about 5 percents) originated from the significant non-coincidence of the functional parameter  $\nu(z)$ . Namely, it is constant, in the case of the model (approximately equal to 0.79), but vary, oscillating from 0.73 to 0.92, being calculated directly from standard atmosphere data  $H(z)$ , differentiating in (10) via the conventional derivative approximation. Estimation of the energy  $E(z)$ , the total energy of all modes at the coordinate range  $[0, z]$ , is given by the following expression

$$E(z) = \frac{1}{2} \int_0^z dz \left( \bar{\rho} V^2 + \frac{p'^2}{\gamma \bar{p}} + \frac{\phi'^2}{\gamma \nu(z) \bar{p}} \right), \quad (76)$$

see the profiles at the Figure 9.

Note, that the energy profiles for the cases of the direct standard atmosphere use and the model, based on explicit linear dependence application gives the curves which difference is scarcely visible (the difference about the percent), hence we propose to use the total energy values and the profiles (76) for the model mode weights estimation.

## 7. Conclusions

The main result of the presented work constitutes in the diagnostic equation, which solution gives the vertical profile of the acoustic mode contribution in the entropy perturbation. This result is illustrated by application to realistic numerical modeling of the atmosphere perturbation by a source positioned near Earth surface. The next result of the study presents the model of the diagnostic algorithm that uses the restricted heights interval, at which the  $H(z)$  dependence is very close to linear. Its restriction guarantees the stability condition and the energy density positively defined. The dependence of explicit approximation on  $z$  allows proceeding with the diagnostic equation solution in explicit form. The resulting diagnostic operations are compared with ones of numerical calculations at the whole available heights range under consideration. The extracted acoustical and entropy modes contributions in perturbation of the gas entropy profiles are plotted and compared with the models'.

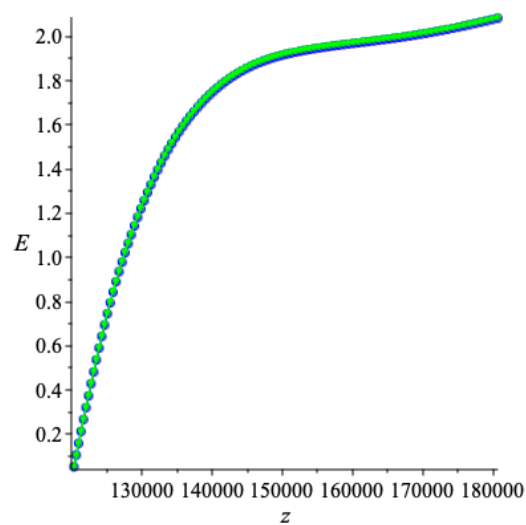


**Figure 9.** Energy calculated by the equation (76) for the cases of standard atmosphere (in blue) and linear dependence (in green) of the height scal  $H(z)$  for  $z \in [120; 180]$  km., see the relation (27).

One of the important ingredients of diagnostics is the possibility to estimate the relative weight of a mode contribution. It is also important to evaluate an error of this estimation, cumulative measurements errors and the theoretical and numerical discrepancies. Such possibility is directly based on the energy density definition with the positive functional parameter  $nu$  at a height range under consideration. It, as known, leads to the norm definition in a functional space of the state vector.

**Author Contributions:** Conceptualization, S.L., methodology, S.L.; software, E.S.; validation, S.L., E.S.; formal analysis, S.L., E.S.; investigation, S.L.; resources, S.L., E.S.; data curation, E.S.; writing—original draft preparation, S.L.; writing—review and editing, S.L., E.S.; visualization, E.S.; supervision, S.L.; project administration, S.L.; All authors have read and agreed to the published version of the manuscript.

**Acknowledgments:** The authors are thankful to Ivan Karpov for important advice and Julia Kurdyaeva for the share of numerical simulation data.

**Conflicts of Interest:** The authors declare no conflict of interest.

## References

1. Kovasznay, Leslie S. G. (1953). "Turbulence in Supersonic Flow". *Journal of the Aeronautical Sciences*. 20 (10): 657–674. doi:10.2514/8.2793. 1953
2. Chu, Boa-Teh; Kovásznay, Leslie S. G. (1958). "Non-linear interactions in a viscous heat-conducting compressible gas". *Journal of Fluid Mechanics*. 3 (5): 494. doi:10.1017/S0022112058000148. 1958
3. Brekhovskikh, L.M.; Godin A.O. *Acoustics of layered media*; Springer-Verlag, Berlin, 1990.
4. Pedloski, J. *Geophysical fluid dynamics*; Springer-Verlag, New York, 1987.
5. Gordin, A.V. *Mathematical problems of hydrodynamical weather prediction. Analytical aspects*; Gydrometeoizdat [in Russian], Leningrad, 1987.
6. Leble, S.B. *Nonlinear waves in waveguides with stratification*; Springer-Verlag, Berlin, 1990.
7. Wu, Y.; Llewellyn Smith, S.; Rottman, J.; Broutman, D.; Minster, J. The propagation of tsunami-generated acoustic-gravity waves in the atmosphere. *J. Atmos. Sci.* 2016, 73, 3025–3036, doi:10.1175/JAS-D-15-0255.1.
8. Leble, S.; Perelomova, A. *Dynamical projectors method in hydro- and electrodynamics*; CRC Press, Taylor and Frensis group, 2018.
9. Zettergren, M.D.; Snively, J.B. Ionospheric response to infrasonic-acoustic waves generated by natural hazard events, *J. Geophys. Res. Space Phys.* 2015, 120, 8002–8024, doi:10.1002/2015JA021116.
10. Leble, S.; Perelomova A. Problem of proper decomposition and initialization of acoustic and entropy modes in a gas affected by the mass force, *Applied Mathematical Modelling* 2013, 37, 629–635.
11. Belikovich, V.V.; Benediktov, E.A.; Tolmacheva, A.V.; Bakhmet'eva, N.V. *Ionospheric Research by Means of Artificial Periodic Irregularities*; Copernicus GmbH: Katlenburg-Lindau, Germany, 2002.

12. Bakhmetieva, N.V.; Grigor'ev, G.I.; Tolmacheva, A.V. Artificial periodic irregularities, hydrodynamic instabilities, and dynamic processes in the mesosphere-lower thermosphere, *Radiophys. Quantum Electron.* **2011**, *53*, 623–637.
13. Leble, S.; Vereshchagin, S.; Bakhmetieva, N.; Grigoriev, G. On the Diagnosis of Unidirectional Acoustic Waves as Applied to the Measurement of Atmospheric Parameters by the API Method in the SURA Experiment, *Atmosphere* **2020**, *11*, 924.
14. Leble, S.; Vereshchagin, S.; Vereshchagina, I. Algorithm for the Diagnostics of Waves and Entropy Mode in the Exponentially Stratified Atmosphere, *Russian Journal of Physical Chemistry B* **2020**, *14* (2), 371–376.
15. Leble, S.; Vereshchagina, I. Problem of disturbance identification by measurement in the vicinity of a point, *TASK QUARTERLY* **2016**, *20*(2) 131–141.
16. Butler, A. H.; Sjoberg, J. P.; Seidel, D. J.; Rosenlof, K. H. A sudden stratospheric warming compendium, *Earth System Science Data* **2017**, *9* (1), 63–76.
17. Karpov, I.V.; Kshevetsky, S.P.; Borchevskina O.P.; Radievsky A.V.; Karpov A.I. Disturbances of the upper atmosphere and ionosphere caused by acoustic-gravity wave sources in the lower atmosphere, *Russian Journal of Physical Chemistry B* **2016**, *10*(1), 127–132.
18. Kshevetskii, S.P.; Kurdyaeva, Y.A.; Gavrilov, N.M.; Karpov, I.V. Simulation of Vertical Propagation of Acoustic-Gravity Waves in the Atmosphere based on Variations of Atmospheric Pressure and Research of Heating of the Upper Atmosphere by Dissipated Waves, *Proceedings of V International conference Atmosphere, Ionosphere, Safety* **2016**, 468–473.
19. Kshevetskii, S.P.; Kurdyaeva, Yu.A. The Numerical Study of Impact Of Acoustic-Gravity Waves from the Pressure Source on The Earth's Surface on the Thermosphere Temperature, *Trudy' Kol'skogo nauchnogo czentra RAS* **2016**, *4*(38), 161–166.
20. Kurdyaeva, Y.A.; Kshevetski, S.P.; Gavrilov, N.; Kulichkov, S.N. Correct boundary conditions for the high-resolution model of nonlinear acoustic-gravity waves forced by atmospheric pressure variations, *Pure and Applied Geophysics* **2018**, *175*, 3639–3652.
21. Brezhnev, Yu.; Kshevetsky, S.; Leble, S. Linear initialization of hydrodynamical fields, *Atmospheric and Oceanic Physics* **1994**, *30*(10), 84–88.
22. Sun, L.; Robinson, W. A.; Chen, G. The predictability of stratospheric warming events: more from the troposphere or the stratosphere?; *Journal of the Atmospheric Sciences* **2012**, *69*(2), 768–783.
23. Perelomova, A. Weakly nonlinear dynamics of short acoustic waves in exponentially stratified gas, *Archives of Acoustics* **2009**, *34* (2), 127–143.
24. *U.S. Standard Atmosphere*, U.S. Government Printing Office, Washington, D.C., 1976.
25. Leble, S.; Perelomova, A. Decomposition of acoustic and entropy modes in a non-isothermal gas affected by a mass force, *Archives of Acoustics* **2018**, *43*(3), 497–503.
26. Leble, S.; Smirnova, E. Tsunami-Launched Acoustic Wave in the Layered Atmosphere: Explicit Formulas Including Electron Density Disturbances, *Atmosphere* **2019**, *10*, 629.
27. Perelomova, A. Nonlinear dynamics of directed acoustic waves in stratified and homogeneous liquids and gases with arbitrary equation of state, *Archives of Acoustics* **2000**, *25* (4), 451–463.
28. Perelomova, A. Nonlinear dynamics of vertically propagating acoustic waves in a stratified atmosphere, *Acta Acustica* **1998**, *84*, 1002–1006.
29. AtmoSym: A multi-scale atmosphere model from the Earth's surface up to 500 km. <http://atmos.kantiana.ru>. 2016. Accessed 10 Apr 2017.